Journal of Neuroscience Methods 268 (2016) 56–65

Contents lists available at ScienceDirect

Journal of Neuroscience Methods

journal homepage: www.elsevier.com/locate/jneumeth

Model of minor stroke with mild peri-infarct ischemic injury

Ursula I. Tuor[a,b,*], Qinbo Deng[a], Dave Rushforth[b], Taduesz Foniok[b], Min Qiao[a]

[a] Department of Physiology and Pharmacology, Cumming School of Medicine, University of Calgary, Calgary, AB T2N 4N1, Canada
[b] Experimental Imaging Centre, Cumming School of Medicine, University of Calgary, Calgary, AB T2N 4N1, Canada

HIGHLIGHTS

- Few animal models can produce a mild ischemia, minor stroke and its recurrence.
- A minor photothrombosis was developed to produce small cortical infarcts.
- This minor stroke was accompanied by a peri-infarct region of mild ischemic injury.
- A minor recurrent stroke was produced by repeating the mild photothrombosis.
- T_2 magnetic resonance imaging was key to identify regions of mild ischemic injury.

ARTICLE INFO

Article history:
Received 7 December 2015
Received in revised form 4 April 2016
Accepted 28 April 2016
Available online 29 April 2016

Keywords:
Photothrombosis
Peri-infarct
Mild ischemic injury
Magnetic resonance imaging

ABSTRACT

Background: Transient ischemic attack, minor stroke and stroke recurrence need improved treatment but lack animal models for research. The aim was to modify photothrombosis methods thereby producing both a minor stroke (with adjacent mild damage) or a minor recurrent stroke.
New method: A minor stroke, as detected using magnetic resonance imaging and histology, was produced using a low intensity beam of white light with a bright centre, a low dose of Rose Bengal and a short 5 min illumination of thinned skull. A recurrent minor stroke was produced by repeating the procedure two days later except the cortical mask was positioned 1.5 mm posteriorly.
Results: The minor photothrombosis procedure produced a small superficial infarct surrounded by a region of scattered necrosis detected histologically. Marked hyperintensities in diffusion weighted and T_2 images identified the infarct. Peri-infarct regions with modest T_2 increases corresponded to regions of scattered cell death. A recurrent minor photothrombosis produced additional damage in regions with overlapping mild injury.
Comparison with existing methods: Previous photothrombosis methods usually produce large cortical infarcts with little penumbra. The current method produces small infarcts with diffuse mild peri-infarct ischemic injury that can be diagnosed using T_2 imaging.
Conclusions: The modified photothrombotic procedure will produce a minor stroke consisting of a small infarct in a region with marked diffusion and T_2 hyperintensities and a peri-infarct region of selective necrosis with modest T_2 changes. Minor recurrent stroke is readily produced but imaging is key for assessing size and location of each insult.

1. Introduction

Minor stroke or TIA is relatively common and often precedes major stroke (Easton et al., 2009; Kernan et al., 2014). Mild transient focal cerebral ischemia, as occurs with a TIA, can be produced experimentally by brief direct occlusion of the middle cerebral artery to produce selective cell necrosis (Ejaz et al., 2015; Qiao et al., 2009). Such mild episodes of cerebral ischemia are not necessarily associated with MR changes. In addition to potential mild ischemic changes, patients with TIA, despite functional recovery, often have small Dw lesions indicative of minor stroke (Brazzelli

Abbreviations: Dw, diffusion weighted; MRI, magnetic resonance imaging; Iba1, Ionized Calcium-Binding Adapter Molecule 1; T_{2w}, transverse relaxation time weighted; TIA, transient ischemic attack.

* Corresponding author at: Teaching, Research and Wellness Building, Room P2E36, 3280 Hospital Drive N.W., Calgary, Alberta T2N 2T8, Canada.
E-mail addresses: utuor@ucalgary.ca (U.I. Tuor), dengqinbo@gmail.com (Q. Deng), drushfor@ucalgary.ca (D. Rushforth), tfoniok@ucalgary.ca (T. Foniok), mqiao@ucalgary.ca (M. Qiao).

http://dx.doi.org/10.1016/j.jneumeth.2016.04.025

et al., 2014). How frequently this is accompanied by peri-infarct tissue with milder ischemic injury is not clear but there are reports of atrophy following TIA and minor stroke (Li et al., 2015; Weiller et al., 1993) indicating that despite good functional recovery there may be diffuse ischemic damage difficult to detect with MR imaging. Furthermore, minor stroke and TIA are predictive of stroke recurrence; and, as an increasing proportion of our population ages the incidence of TIA, minor stroke and recurrent stroke is anticipated to increase. However, their diagnosis, pathophysiology and management remains suboptimal with effective treatment options limited to thrombolytic or endovascular therapy.

A factor curbing advances in this area of stroke research is that there are relatively few simple animal models of minor and recurrent stroke available. Photothrombosis is a relatively simple method technically for producing rather non-invasively a focal infarct in experimental animals (Watson et al., 1985). However, the majority of previous studies using photothrombosis have produced rather large focal infarcts throughout the entire cortex that often include subcortical white matter (Dietrich et al., 1987a; Lee et al., 1996; Pierpaoli et al., 1993; Watson et al., 1985). A few studies have produced smaller infarcts or single vessel infarcts using photothrombosis (e.g. (Harrison et al., 2013; Moon et al., 2009; Pevsner et al., 2001; Shih et al., 2013)) and spontaneous reperfusion of thrombosed vessels has been observed (Zhang et al., 2005). However, producing infarction rather than mild ischemic injury in the peri-infarct region has been the focus of such previous studies. The aim of the current study was to investigate the conditions required to produce diffuse mild ischemic injury surrounding a small photothrombotic lesion—an insult that that could then model clinical minor strokes with a penumbra and could also be used to potentially model recurrent minor strokes.

Modifying the intensity and the duration of light illuminating the cerebral cortex following Rose Bengal injection produced small cortical infarcts with peri-infarct regions of scattered necrosis. T_2 imaging facilitated identification of the precise size and location of the small ischemic lesion and its peri-infarct region of mild ischemic injury. The photothrombotic insult could be repeated to produce a recurrent stroke and overlapping regions of mild ischemic damage.

2. Methods

2.1. Animals

The care and handling of all animals were carried out in accordance with the guidelines of the Canadian Council on Animal Care for care and use of experimental animals. Experiments were approved by the University of Calgary Health Sciences Animal Care Committee (Protocol M11017). Male Wistar rats (Charles River, Montreal, Canada) were acclimatized to a 12 h light/dark cycle with free access to food and water. Animals weighed 226–395 g (median 263) at the time of surgery. Following stroke, rats were housed in separate cages with free access to soft and hard food, water and environmental enrichment. All surgical procedures were performed using aseptic techniques.

2.2. Minor photothrombosis model

The photothrombotic stroke method uses a photo-activatable dye, Rose Bengal, to generate coagulation within vessels using experimental conditions that have generally resulted in a relatively large ischemic infarct within the entire depth of the cortex and often also white matter and subcortical structures (Dietrich et al., 1987a; Lee et al., 1996; Pierpaoli et al., 1993). Injection and illumination conditions were chosen to potentially produce minor strokes by selecting conditions that could enhance early platelet disaggregation and thrombus clearance as has been reported to be visualized directly using confocal microscopy (Zhang et al., 2005). Thus the concentration of Rose Bengal (Sigma–Aldrich, St Louis, MO) administered IV (prepared as 10 mg/ml in sterile distilled water and filtered through an 80 μm filter) was low (10 mg/kg, 1 ml/kg) compared to many previous studies using 15–50 mg/kg (Jolkkonen et al., 2007; Pierpaoli et al., 1993; Van Bruggen et al., 1992; Verlooy et al., 1993). The pharmacokinetics of Rose Bengal was used to help select the duration of illumination (Fig. 1A). Rose Bengal levels were measured spectrophotometrically in plasma from timed samples of arterial blood. Concentrations were determined from means of triplicate measures using a standard curve of known Rose Bengal concentrations and absorptions measured at 532 nm. Rose Bengal concentration peaked within the first minute following IV administration, clearing over 10 min (Fig. 1A), similar to observations in the mouse (Boquillon et al., 1992; Zhang and Murphy 2007). Thus, for the duration of illumination, a rather short period of five minutes was selected compared to the 15–30 min periods of illumination used in previous studies (e.g. Jolkkonen et al., 2007; Moon et al., 2009; Pevsner et al., 2001; Pierpaoli et al., 1993; Schroeter et al., 2001; Van Bruggen et al., 1992; Watson et al., 1985).

The animal was prepared to optimize illumination of the cortex under normally maintained physiological conditions. Rats were anesthetized with isoflurane (1.5–2.5% in 30% oxygen remainder nitrogen) to allow restraint of the head in a stereotaxic frame and surgical exposure of the skull. A femoral vein catheter was inserted surgically to allow effective intravenous injection of Rose Bengal. Normothermia (rectal temperature 36.5–37.5 °C) was maintained using a heating pad. Anesthesia was adjusted to maintain normal spontaneous respiration (55–75 breaths/min, mean 65 ± 9) resulting in good oxygenation (>98% saturation) confirmed with pulse oximetry in a subgroup of animals. To limit potential variations in light transmission into cortex, the skull was thinned to translucence over an area somewhat larger than the illumination region using a saline cooled dental drill. Bleeding was controlled using bone wax to provide a clean field of illumination. In some animals, regional cerebral blood flow (rCBF) within the illuminated region was measured prior to and post illumination using laser-Doppler flowmetry (Periflux PF5010, Perimed) with a 1.0 mm probe (403, Perimed) placed perpendicular to the skull. Rectal temperature was monitored and maintained throughout the experiment and for 1 h after surgery confirming that thermoregulation and body temperature was normal. After illumination, surgical sites were closed with 3-0 nylon sutures and buprenorphine (0.03 mg/kg) was administered to provide analgesia.

For photothrombosis, an opaque foil mask with an opening size of 3 mm × 3 mm was fabricated in order to illuminate a region encompassing several 1 mm thick MR slices. This was placed directly on the skull, with the centre of the mask at stereotaxic coordinates of 1.5 mm anteroposterior from bregma and 2.5 mm mediolateral from the midline (Paxinos and Watson 1998). The illumination apparatus used light from a 150 W halogen bulb (NCL 150 illuminator, Volpi) transmitted perpendicularly from the source through an infrared filter (#46-386, Edmund Optics, Barrington, NJ) and a 30 cm length of 13 mm diameter fibre optic cable (Fig. 1B). In initial studies light intensity of illumination was varied from 200,000 to 400,000 lux as measured at the skull (Light Meter, Sper Scientific Ltd.) which is the equivalent of approx. 30–60 mW/cm^2 at 555 nm. Direct comparisons of intensities used between studies are difficult; intensities reported have ranged from 3 to 30 mW or 285 to 580 mW/cm2 for green laser/light (Dietrich et al., 1987b; Harrison et al., 2013; Kao et al., 2014; Zhang et al., 2005) and 100 to 580 mW/cm^2 for white light (Lee et al., 1996; Pevsner et al., 2001).

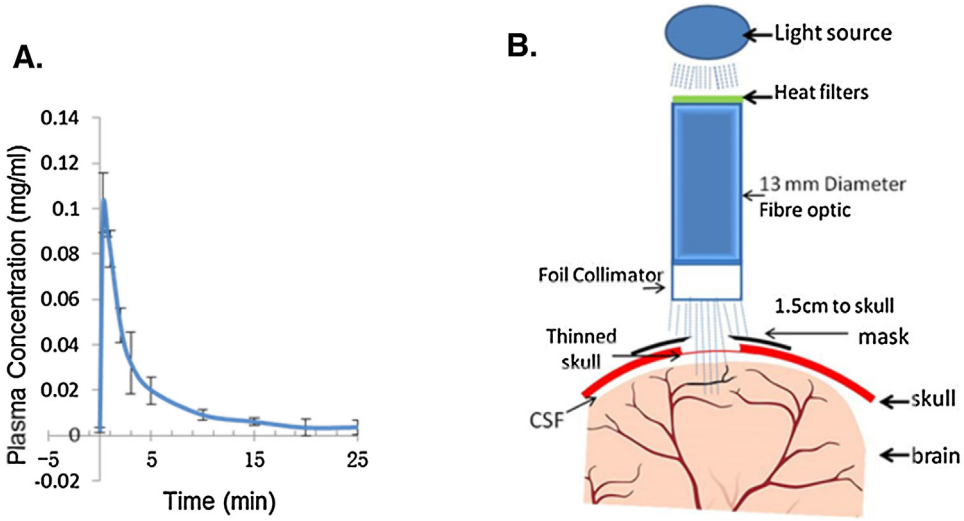

Fig. 1. Production of a mild photothrombotic lesion. (A) Mean arterial plasma concentration at different times following administration of Rose Bengal (10 mg/kg, IV, $n = 3$) demonstrated maximal levels of photochemical dye in blood soon after injection. (B) The method involved using a halogen light source, heat filter and fibre optic cable with foil collimator positioned perpendicular to the thinned skull that was covered with an opaque mask with a 3 mm × 3 mm rectangular opening.

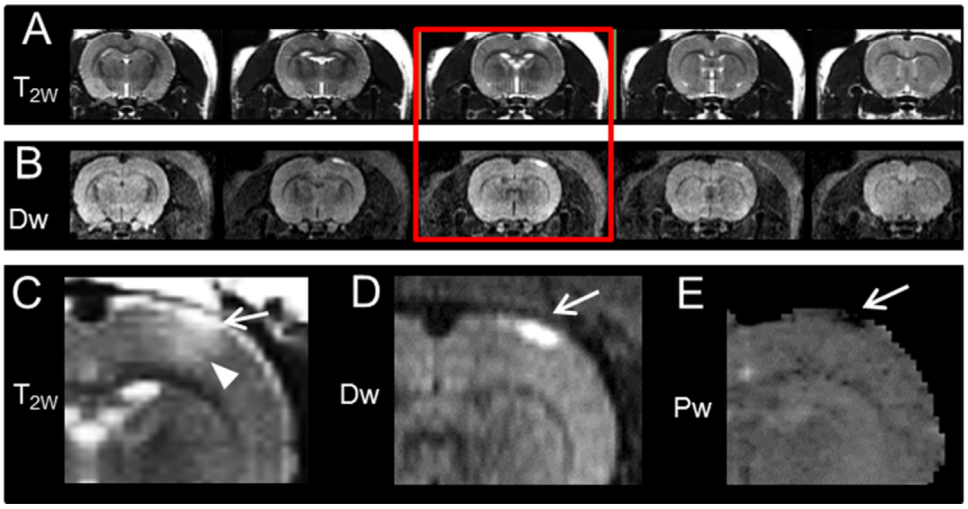

Fig. 2. MR imaging of cerebral cortex 24 h following a minor photothrombotic insult. T_2 weighted (T_{2w}) images (A) or diffusion weighted (Dw) images (B) showed hyperintense cortical changes within different slices through the cerebrum. Perfusion imaging (P_w) was performed in a slice containing the lesions of increased intensity (outlined in red; enlarged in C–E). A modest T_{2w} increase (arrowhead) was evident in the region adjacent to the hyperintense lesion observed in the T_{2w} and Dw images. (For interpretation of the references to colour in this figure legend, the reader is referred to the web version of this article.)

Presently, lesions were generally produced in the right hemisphere. In some experiments the skull was thinned over both the right and left hemispheres and illuminated simultaneously with the light centred at the midline but some lateral variation in lesion size occurred. A 15 mm length of a reflective foil collimator (Fig. 1B) was added to the end of the optic fibre to increase homogeneity of the light intensity over the 13 mm diameter of the fibre. The intensity distribution remained maximal centrally with slight gradations of surrounding lower light intensities. The illumination produced regions of milder ischemic injury posteriorly and anteriorly as detected with MRI (e.g. Fig. 2). In animals in which two photothrombotic insults were produced, the right side was prepared for photothrombosis and the first illumination was followed 2 days later by a second venous cannulation under anesthesia and exposure of the previously thinned skull prior to a second photothrombosis procedure.

2.3. Magnetic resonance imaging (MRI)

To assess ischemic injury, MR scans were acquired the day following a photothrombotic insult to determine the ischemic injury detectable using T_2 or diffusion weighted imaging e.g. Qiao et al. (2004). Rats anesthetized with isoflurane were scanned using a 35 mm quadrature volume radiofrequency coil and a 9.4 T Bruker Biospin MR imaging system with Paravision 5.1 software and Avance II hardware. Each scanning session acquired T_2 weighted (T_{2w}) and diffusion weighted (Dw) images with a 3 cm × 3 cm field of view, a 128 × 128 matrix and at least twenty 0.7 mm thick contiguous slices covering the cerebrum. The T_2 scan (repetition time = 7 s) acquired a set of 32 T_2 weighted images with an inter-echo spacing of 10 ms. A set of diffusion weighted images (repetition time = 5 s, echo time = 40 ms) were acquired with 5 b values (74.5, 292, 655, 891 and 1164 s/mm^2). In a subgroup of animals a perfusion-weighted map was also acquired in a single slice 1 mm thick to determine changes in cerebral blood flow using a continu-

ous arterial spin labelling method (Qiao et al., 2004; Williams et al., 1992). Briefly, within the slice direction and in a plane 2–3 mm distal to the edge of the skull, a 2 s long radiofrequency labelling pulse was applied to the neck vessels in the presence of a 2 G/cm gradient. This was followed with a delay of 400 ms by a HASTE (Half-Fourier Acquisition Single Shot Turbo Spin Echo) sequence using a repetition time of 3 s, effective echo time of 13.3 ms and a RARE factor of 36 for a total of 16 averages. Magnetization in unsaturated control images were obtained by using the same radiofrequency excitation applied symmetrically opposite to the labelling plane to help eliminate magnetization transfer effects. Cerebral perfusion (Williams et al., 1992) was calculated using magnetization measured in regions of interest (i) as a percentage of flow in non-illuminated cortex (c) using:

Flow (%) = $100 \times ((M_i^{control} - M_i^{saturated})/2M_i^{control})/((M_c^{control} - M_c^{saturated})/2M_c^{control})$ and assuming constant values for $T_{1apparent}$ and the partition coefficient for water. The MRI scans were converted to T_2 or perfusion maps using the Bruker software and regions of interest included the outer cortex (lesion), the mid cortex (peri-lesion), the inner third of cortex and a control region within either temporal or homologous contralateral cortex.

2.4. Histology

At 24 h after MR imaging, animals were perfusion fixed with formalin under deep anesthesia and brains were removed and embedded in paraffin. Several coronal sections (6 μm thick) matching the coronal MR images (at least 3–4 MR slices per animal) were stained with hematoxylin and eosin or cresyl violet. Histological sections were registered to MR images according to distinct anatomical features that included matching ventricles and white matter structures. To evaluate the scattered cell death observed following mild ischemic insults, a score for brain injury was assessed blinded to the animal identity similar to that described previously (Qiao et al., 2009). The cortical thickness was divided into 3 areas of outer and mid and inner thirds of cortex. A cumulative score was obtained from the score for each region graded as: 0 for normal, 1 for <10% of cellular injury, 2 for 10–50% of cellular injury, 3 for >50% cellular injury (partial infarct) and 4 for confluent areas of pan-necrosis (infarct). If more than one severity of injury was observed the scores were averaged.

Ischemic cell changes were also investigated using two additional staining methods. Sections with photothrombotic injury were stained for a marker of cell death or degenerating neurons using fluorojade B (Schmued and Hopkins 2000) according to manufacturer's instructions (Histo-Chem, Inc., Jefferson, Arkansas, USA). Briefly, deparaffinised sections were exposed to 0.06% potassium permanganate for 15 min washed in distilled water and then stained with 0.001% fluorojade solution. In addition, early activation of microglia was assessed immunohistochemically using an antibody against Ionized Calcium-Binding Adapter Molecule 1 (Iba1, 1:1000, AB_839504, Wako Chemicals, USA) which is specifically expressed in microglia and is upregulated following cerebral ischemia (Ito et al., 2001). Sections were incubated with 10% goat serum, then primary antibody rabbit anti-Iba1 followed by the secondary antibody, Alexa Fluor® 488 goat anti-rabbit IgG (Thermo Fisher Scientific, Waltham, MA, USA).

2.5. Statistical analysis

All group data is reported as mean ± SD and statistical comparisons were performed using SigmaPlot 13 software (Systat Software Inc., San Jose, CA) and differences were considered significant at $P < 0.05$. Differences between multiple groups were analysed using an analysis of variance (ANOVA) or a repeated ANOVA for repeated measures, followed by a Student Neuman–Keul's test for a multiple comparison of groups. Comparisons of the difference of means between two groups used a Student's *t*-test. For the investigation of the relationship between illumination intensity and ischemic lesion volume a Pearson product correlation analysis was performed. Histology scores were compared using an ANOVA on ranks followed by a Rank Sum Test.

3. Results

3.1. Mild ischemic injury produced with the minor photothrombotic method

In the first experiments, light intensity was varied. These experiments demonstrated that 5 min illumination with a low light setting (approx. 280,000 lux) at the illuminated area produced smaller T_2 lesions than more intense light levels. Similar to reports in the literature (Alaverdashvili et al., 2008; Kao et al., 2014), the intensity of light correlated to volume of damage ($n = 15$, $R = 0.86$, $P < 0.0002$, Pearson correlation). Thus, for production of a minor photothrombotic lesion, we subsequently focused on illuminating with a light intensity of 280,000 lux at the skull (approx. 41 mW/cm^2 at 555 nm) for 5 min starting at 1 min following bolus injection. For each light source, optic fibre and filter configuration, this optimal light intensity will likely need to be confirmed empirically. Note that centring the light fibre on the mask and positioning the fibre perpendicular to the skull were important factors affecting lesion induction along with spatial distribution of the light intensity. It is prudent to confirm central light intensity routinely thereby avoiding potential variations (e.g. 25% increased central intensity with replacement of an ageing halogen bulb). Light intensity, after a warming period, was relatively stable over 5 min of illumination (coefficient of variation of 1.2%) and stable after initial bulb replacement (e.g. range of 41–44 mW/cm^2 without decline over 3 months); with some light sources stabilizers have been used and are important for maintaining constant illumination (Alaverdashvili et al., 2015; Verlooy et al., 1993).

With our minor photothrombotic procedure, ischemic changes detected in T_{2w} (e.g. Fig. 2A) and Dw (e.g. Fig. 2B) images consisted of lesions in multiple slices detected as marked hyperintensities in the superficial cortex. The central slice had the largest areas of superficial hyperintensity changes. Within the perfusion weighted scan of the central slice, the regions of marked hyperintensity (Fig. 2C and D) corresponded to an area of marked hypoperfusion (Fig. 2E). Adjacent to the marked hyperintense regions of T_{2w}, there were more modest increases in T_2 corresponding to regions with either slight or little apparent reduction in cortical perfusion. Of 23 consecutive animals subjected to conditions to produce a minor photothrombosis, one died during surgery and one had no MR changes. The majority (14/21) had small infarcts with mild/minor lesions (mean volume of 1.7 ± 0.8 mm^3) and the remainder had somewhat larger infarcts with moderate lesions (total volume of 5.9 ± 1.8 mm^3) overlying regions with mild T_2 changes.

3.2. Variablity in lesion size and the cerebral perfusion changes

To analyse similar lesion sizes, the Dw lesions in each slice selected for analysis were classified according to their size: i.e. mild (no lesion or slight superficial spot <0.7 mm^2), minor (superficial lesion 0.8–2.5 mm^2) and moderate (2.5–6 mm^2) (e.g. Fig. 3A, a–c). Irrespective of the Dw lesion size, modest T_2 intensity increases were also observed in cortex adjacent to the Dw/T_2 hyperintense core (arrow heads, Fig. 3A, d–f). laser Doppler flowmetry changes measured immediately post-illumination (Fig. 3B), within a region likely encompassing both photothrombotic and non-affected cortex, tended to show recovery towards baseline after the end of

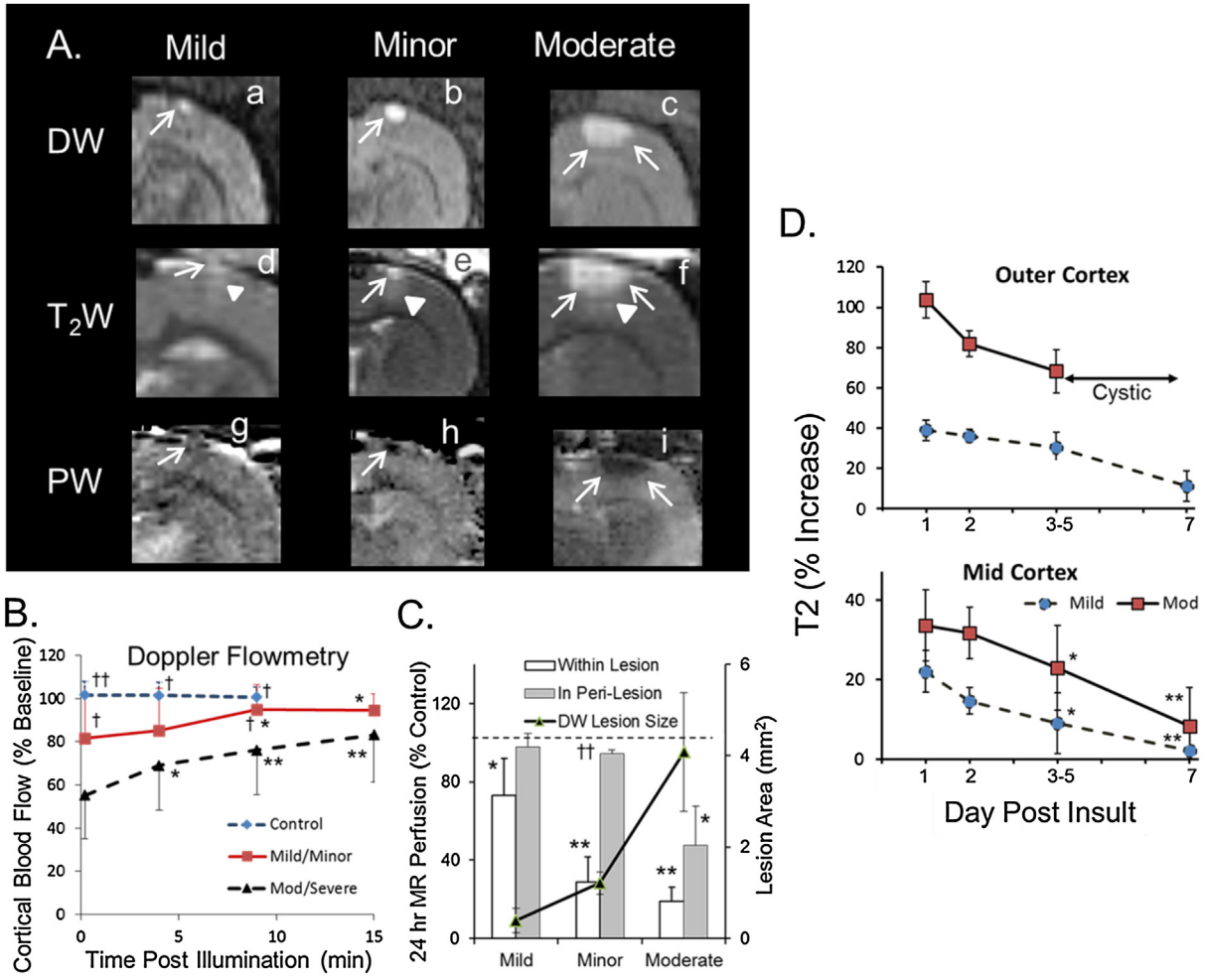

Fig. 3. MR imaging assessment of differing severities of photothrombotic lesions 24 h following illumination. (A) Representative diffusion weighted (Dw) images (a–c), T_2 weighted (T_{2w}) images (d–f) and perfusion weighted (PW) images (g–i) following a mild, minor or moderate photothrombotic insult. Marked altered intensities occur within the ischemic lesion (arrows) and modest changes in adjacent regions (arrowhead). (B) Cortical blood flow changes measured using Doppler flowmetry in control animals without illumination ($n = 5$) and animals with mild/minor ($n = 7$) or moderate/severe ($n = 8$) lesions indicating a decrease in flow post-illumination with some recovery in animals with smaller ischemic lesions. $^{*}P < 0.01$, $^{**}P < 0.001$, different from baseline; $^{+}P < 0.01$, $^{++}P < 0.001$ different from moderate/severe group. (C) Mean perfusion (% of normal control cortex) within lesions of mild ($n = 5$), minor ($n = 4$) or moderate ($n = 4$) severity demonstrating marked hypo-perfusion within the diffusion weighted (Dw) lesion area and less marked perfusion deficits in adjacent mid peri-lesion areas. $^{*}P < 0.05$, $^{**}P < 0.005$, different from control; $^{+}P < 0.05$, $^{++}P < 0.005$ different from mid peri-lesion region (paired Student's *t*-test). (D) In animals imaged at 1d and at various additional times, the T_2 increase (% control) declined over time for either moderate or mild lesions ($n = 11$, 4, 5, 4 and 10, 3, 5, 4 for the 1, 2, 3–5, and 7 day points, respectively). $^{*}P < 0.01$, $^{**}P < 0.001$, different from 1 day post insult.

illumination and the recovery was greater in animals with mild MR lesions compared to those with larger lesions. In cerebral perfusion images acquired using MRI at 24 h post photothrombosis, (Fig. 3A, i–k) there was persistent marked hypoperfusion in all lesion regions (arrows) and flow reductions were substantial in moderate but not mild lesions (Fig. 3C). Quantitative assessment of perfusion in cortex adjacent to the lesions was significantly reduced in moderate but not mild or minor MR lesions.

3.3. Longitudinal changes in T_2

In order to help characterize the cerebral effects of mild or moderate photothrombotic lesions, the T_2 changes were assessed at different time points in additional animals that were imaged at 1d post and then at one or more additional time points up to 7d later (Fig. 3D). T_2 in both the lesion (outer cortex) and adjacent peri-lesion (mid cortex) increased relative to control cortex with increases in the moderate lesions exceeding those of the mild lesions ($P < 0.001$). The T_2 changes decreased over the first few days as edema resolved ($P < 0.01$) (2 way ANOVA with Holm Sidak test). Cystic formation occurred in the superficial cortex by 5–7 days resulting in very high T_2 (not shown as cortical tissue was lost) whereas there was a normalization of T_2 within the mid cortex.

3.4. Histological changes corresponding with MR changes

Investigation of the histological correlates of the changes in the MR images generally demonstrated a good correspondence between severity of ischemic injury (Fig. 4A, a–d and B, a–c) and T_2 changes at 1d post-insult (Fig. 4A, e). Both hematoxylin and eosin and cresyl violet stained sections showed extensive loss of neurons and a developing infarct within the T_2 lesion of marked hyperintensity (T_2 generally greater than 150% control). In regions of deep cortex adjacent to and surrounding the infarct there were regions of scattered necrosis or selective neuronal necrosis that, in the corresponding MR slices, reflected modest increases in T_2 (approx. 115–150%). Minimal T_2 increases (e.g. 10–15%) could be observed without apparent signs of ischemic tissue injury, particularly in deeper cortical layers. Also infrequently, small infarcts were observed in superficial cortex histologically without visible hyperintense Dw/T_2 lesions detectable in MR images. Such discrepancies between imaging and histological changes were considered

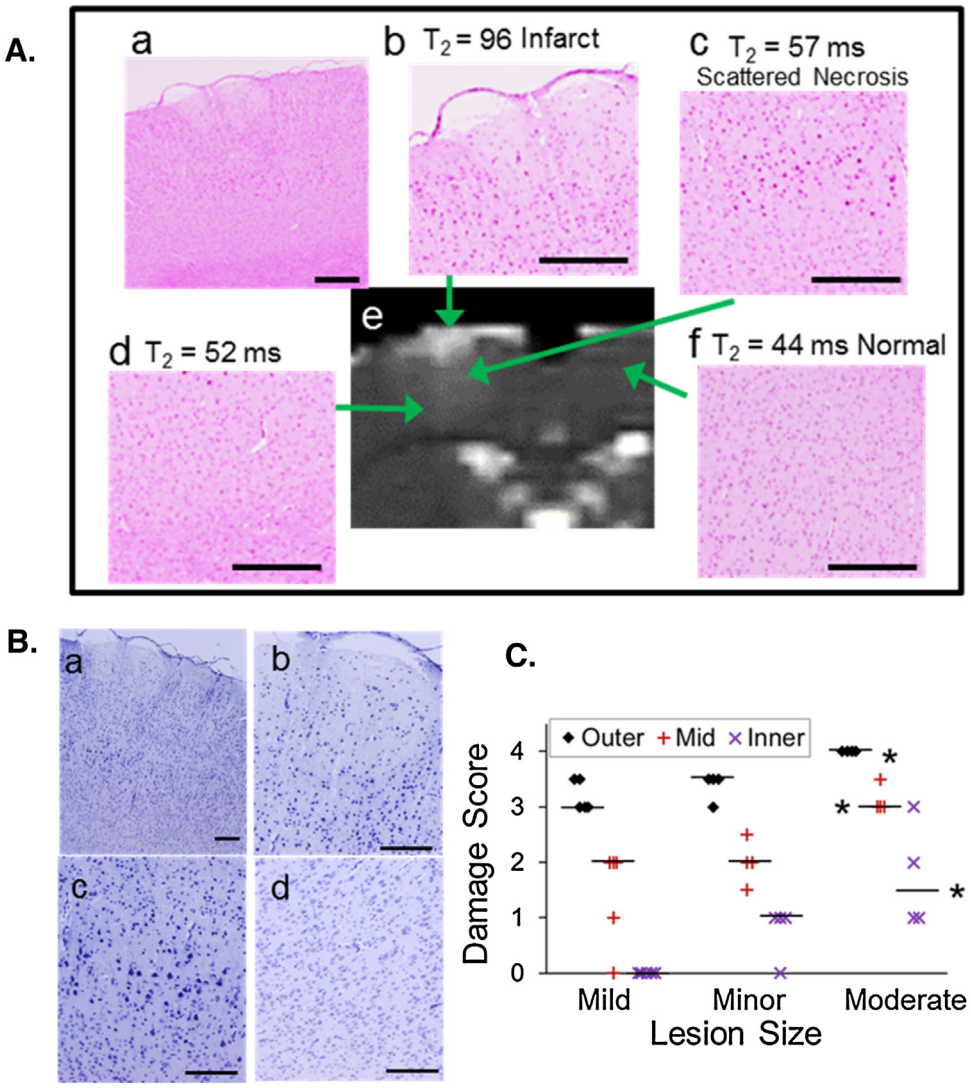

Fig. 4. Representative histological section containing a minor photothrombotic lesion and the T_2 measures within these regions selected from the corresponding T_{2w} MR slice (A—e). (A) Hematoxlyin and eosin stained section (a) and magnified subregions (b–d) and their T_2 measures along with a normal control region (f) for comparison. A marked T_2 increase (e.g. >50%) within the lesion (b) was associated with infarction whereas within mid or inner cortex a modest increase in T_2 (approx. 15–50%) corresponded to a region with scattered cell death (c,d). (B) Cresyl violet stained section (a) and magnified subregions (b–d) matching the hematoxylin and eosin stained sections (b,c,f) that also demonstrate the presence of pannecrosis (b) and scattered necrosis (c) within the cortex. Scale bar = 200 μm. (C) Damage score assessed for mild ($n = 5$), minor ($n = 4$) or moderate ($n = 4$) lesions within outer, mid and inner levels of cortex. *$P < 0.02$, moderate different from mild for corresponding depth of cortex.

to be due to differences in sensitivity and spatial resolution of the two methods; the 0.7 mm thick MR slice reflecting a tissue average of 6 μm histology sections. For sections with a good registration of the T_2 lesion and histology, blinded grading of the injury in hematoxylin and eosin stained sections at 1 or 2 days after the photothrombotic insult demonstrated greater ischemic injury in moderate than mild T_2 lesions at all depths of cortex (Fig. 4C). Infarction or extensive necrosis occurred within the lesion in outer cortex with more modest to minimal changes at mid and inner levels, respectively ($P < 0.001$). In a subset of animals (3 per lesion severity) additional indications of mild ischemic injury were observed in adjacent sections stained with fluorojade and Iba1 (e.g. Fig. 5). In these animals, within mid and inner cortex, there were scattered necrotic or degenerating neurons stained with fluorojade (e.g. Fig. 5B–D) and these regions were associated with modest hyperintense T_2 changes. In addition, in regions with modest T_2 hyperintensity, microglia stained with Iba1 were generally larger and of a bushy morphology (Fig. 5E–G) compared to microglia in control cortex (Fig. 5H).

3.5. Brain damage with a recurrent minor photothrombotic insult

We also investigated the ability to produce multiple minor photothrombotic insults as a novel model of recurrent minor stroke. For stroke recurrence, the mild photothrombotic model producing a minor stroke (Fig. 6A) was repeated 2 days later ($n = 4$). The skull was re-exposed and Rose Bengal was injected followed by illumination of the cortex—with one difference being that the mask over the skull was positioned 1.5 mm more posterior than the initial insult (Fig. 6B). The first insult of minor stroke that was produced had several slices with modest T_2/Dw ischemic changes, particularly in the most anterior and posterior slices (e.g. Fig. 6A). With a second illumination two days later, the most anterior slice did not receive another ischemic insult and thus there was some recovery towards normal in the T_2 change within the lesion (Fig. 6C), similar to that reported in Fig. 3D. With an overlap in illumination in the initial mild posterior slice, there was evidence of additional damage and T_2 augmentation. The new most posterior slice with the second illumination had only a single insult and mild T_2 changes.

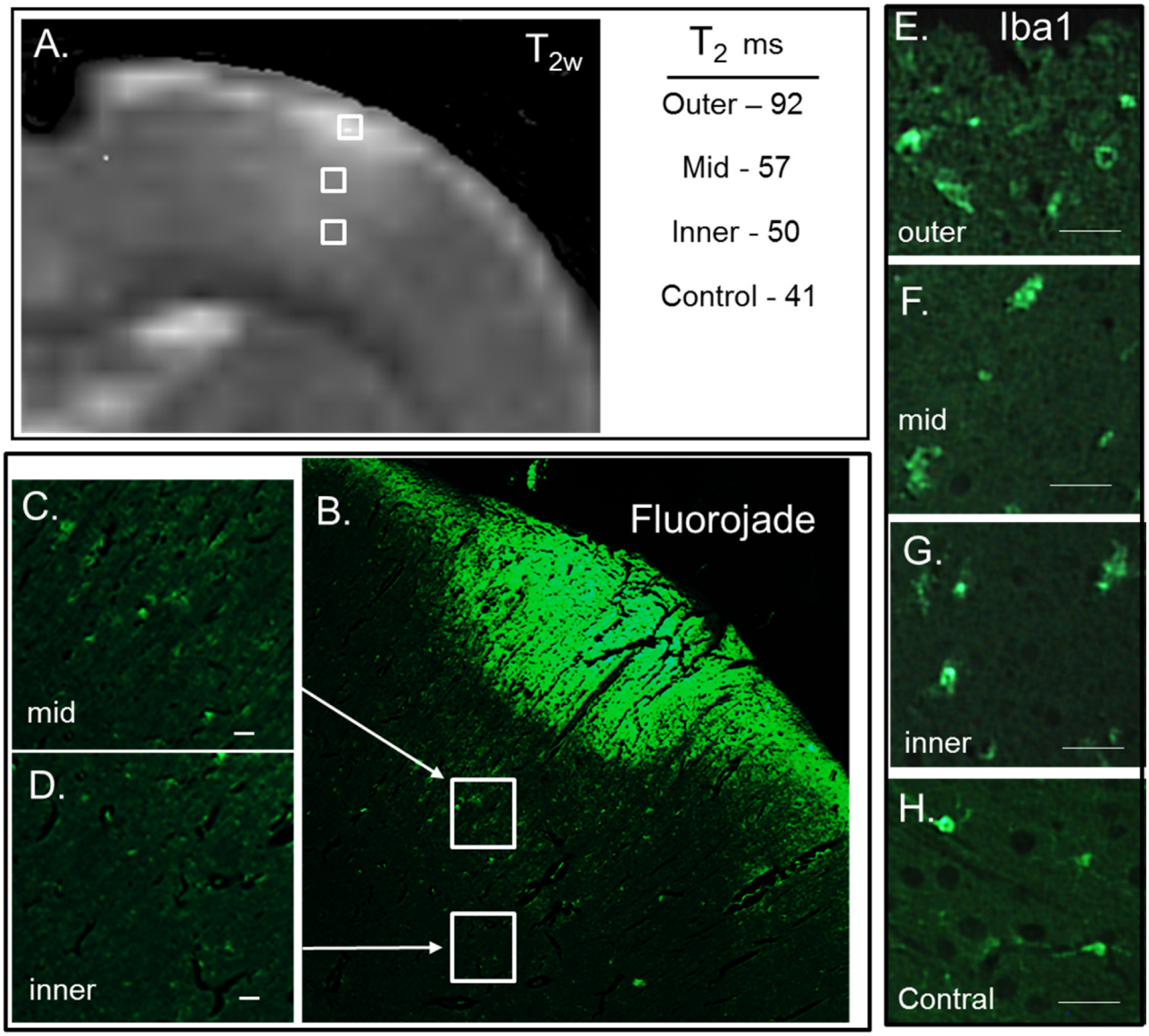

Fig. 5. Ischemic injury in regions of modest hyperintense T_2 changes. (A) A T_2 weighted MR image of a representative animal with a minor photothrombotic lesion showing modest T_2 hyperintensity within mid and inner cortex. (B) A corresponding section stained with fluorojade indicating increased degenerating or necrotic cells within the lesion and within mid (C) or inner (D) depths of cortex. Within a corresponding section stained with Iba1 there were increased numbers of ramified microglia in outer (E), mid (F) and inner (G) cortex compared to microglia in contralateral uninjured cortex (H). Scale bar = 25 μm.

Histologically this corresponded to a median damage score of 5.5 (range of 3–6) for the single mild injury and a median score of 7 (range of 7–9) for the double injury slice ($P < 0.03$, Mann–Whitney Rank Sum Test). Although additional injury was detectable with the use of MRI, the actual number of slices and severity of injury in each slice along with the number of slices with overlap varied so that MRI was important for identifying insult severity and location when producing recurrent insults.

4. Discussion

4.1. Production of a minor cerebral photothrombotic lesion

Photothrombosis has traditionally been used to produce consistent rather large infarcts within the cortex and similar to the present study, MR imaging changes of increased T_2 and Dw within the infarct lesions have been reported previously (Pierpaoli et al., 1993; Van Bruggen et al., 1992). Similar to the present results, a reduction in T_2 from maximal values at 1–2d post insult has been reported to occur during resolution of edema within the lesion by others (Jolkkonen et al., 2007; Schroeter et al., 2001). Two different studies have also reported the production of smaller infarcts using white light. One provided evidence for some penumbra or transition zone of milder ischemic changes acutely whereas the other investigated chronic histological changes and observed cortical thinning and brain atrophy (Moon et al., 2009; Pevsner et al., 2001). The very small infarct size of less than 3.0 mm^3 in the current study is generally smaller than that of Moon et al. (2009) (1.16–6.43 mm^3) and markedly less than the majority of studies using standard photothrombosis (e.g. infarct volumes of 15–100 mm^3) (Jolkkonen et al., 2007; Kao et al., 2014; Lee et al., 1996). Even smaller infarcts (approx. 0.2 mm^3) can be produced by *permanent* occlusion of single cerebral vessels using focused beams of green laser light (Harrison et al., 2013; Shih et al., 2013). However, mild peri-infarct ischemic changes have generally not been investigated and/or reported in these studies.

MR imaging and histological characteristics of such mild insults producing small infarcts with hyperintense T_2 and Dw lesions have

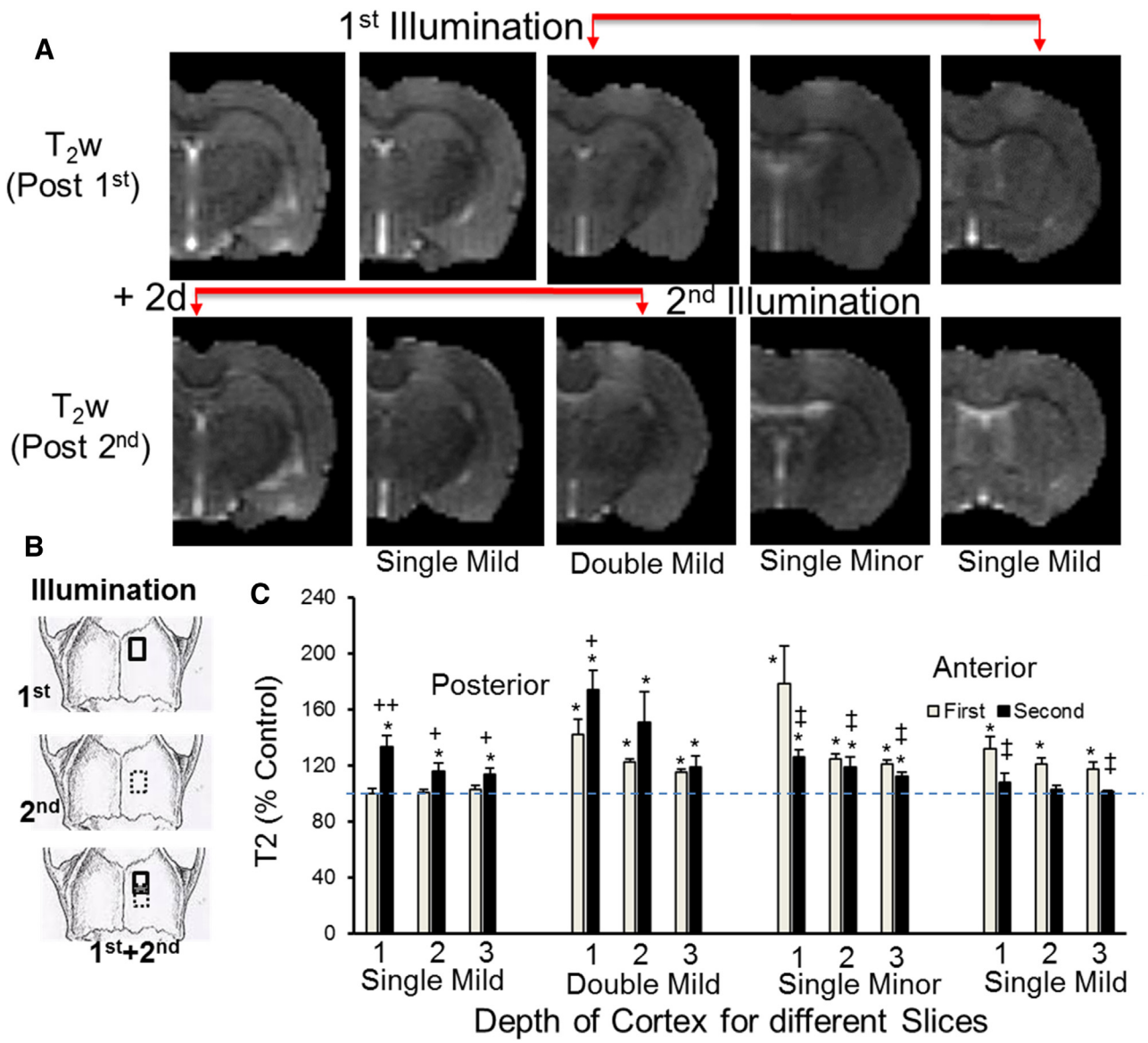

Fig. 6. Effects of a recurrent minor photothrombosis. (A) T_{2w} MR slices demonstrating ischemic changes 24 h after a minor photothrombosis (top panel). Also shown (lower panel) are the T_{2w} changes 24 h following a second minor photothrombosis produced 2d later in the same animal. Ischemic T_2 changes from single insults are observed in the two anterior slices (from the first insult) and the posterior slices (from the second insult) whereas T_2 changes from a double insult are observed in a central slice. (B) The sketch demonstrates that the position of the mask for illumination was moved 1.5 mm posterior between the first and second procedure resulting in an overlap of illumination and a double photothrombotic insult in mid-slices. (C) Quantitative measures of the T_2 increases for 3 different depths of cortex – 1. outer, 2. mid and 3. inner – within 4 different MR slices. Following the first insult, anterior slices have significant increases in T_2, whereas following the second photothrombosis such T_2 increases are observed in posterior slices. In the slice with overlap and a double insult the T_2 increase is enhanced following the second photothrombosis. $^{*}P < 0.003$ different from control cortex; $^{+}P < 0.05$, $^{++}P < 0.005$, increased from 1st insult; $^{\ddagger}P < 0.05$ decreased from 1st insult (paired Student's Bonferroni corrected *t*-test).

not been well characterized. Novel to our study is the observation that following a minor photothrombotic insult, regions with scattered necrosis generally had modest T_2 increases but lacked either diffusion weighted changes or major reductions in perfusion at 24 h post-insult. Modest T_2 changes appeared to be within a region with transient thrombotic vessel occlusion as indicated by the recovery of reductions in laser Doppler flowmetry post-illumination and are consistent with a reported spontaneous recannalization observed following photothrombosis (Zhang et al., 2005). Doppler flow not returning to pre-lesion baseline values likely reflect persistent ischemia in the core lesion as was observed in the MR perfusion scans. Similar substantial and persistent flow reductions have been commonly observed in the locus of major photothrombotic insults (Gu et al., 1999; Kao et al., 2014; Schoknecht et al., 2014). Thus, this minor photothrombosis provides a technically straightforward method with relatively low invasiveness for producing modest flow reductions and mild ischemic injury; an insult which provides a promising target for investigating new treatments. Such mild ischemic injury may be relevant not only to TIA and minor stroke but also for vascular dementia and ageing for which animal models are limited. T_2 imaging provides a non-invasive method for assessing the extent of the infarct (not amenable to treatment) and mild ischemic changes (potentially amenable to treatment) prior to randomization for testing new therapies promoting neuroprotection or repair.

4.2. Limitations of the minor photothrombotic stroke model

There are several limitations of the current study regarding the production of the minor photothrombotic insult. Despite

standardizing many of the procedures there remained some variability in the lesion sizes so that MRI scanning was useful to confirm the severity and exact location of the small infarcts produced. A degree of variability in lesion size may be unavoidable for a number of reasons. The relatively low illumination intensity to produce a mild insult may be near a threshold where modest differences in Rose Bengal pharmacokinetics and angle/intensity of light illumination affect efficacy of photothrombosis and infarct size. In addition, the exact location of the small infarcts is likely affected by anatomical variations in the pial vasculature producing localized differences in thrombi production and their spontaneous dissolution. However, some of these limitations might be overcome by designing the light source so that it provides a well characterized stable intensity of light illuminating the cortex within a range of intensities sufficient to produce mild photothrombosis. Also, adding additional imaging, such as laser speckle perfusion imaging to identify the duration and distribution of microvascular occlusion or the degree of hypoperfusion, as might occur with small vessel disease, could help further standardize methods, reduce variability and/or allow appropriate selection of animals for drug therapy studies.

Another limitation may be that the MR imaging responses observed, which are useful to diagnose mild ischemic injury, may be specific to the mild photothrombotic model. Modest T_2 increases in perinfarct regions reflected mild damage associated with mild ischemic cellular changes. This differs from transient ischemia induced by clip occlusion of the middle cerebral artery where no T_2 or Dw changes have been observed 24 h later despite mild ischemic changes histologically. The modest T_2 changes provide evidence for early vasogenic edema which is not unexpected considering that Rose Bengal interacts with light to produce single oxygen species resulting in damage to the endothelium followed by vasoconstriction, platelet aggregation and production of thrombi (Dietrich et al., 1986; Watson et al., 1985). Indeed, photothrombotic insults are accompanied by increases in blood–brain barrier permeability (Dietrich et al., 1987a) with blood–brain barrier dysfunction in peri-infarct regions observed acutely and chronically (Reeson et al., 2015; Schoknecht et al., 2014). However, with large photothrombotic lesions, the peri-infarct region is narrow (<500 μm) and appears to be accompanied by marked gradations of hypoperfusion or ischemia (Schoknecht et al., 2014) whereas our model of minor photothrombosis is associated with only mild ischemia and modest T_2 changes reflecting some blood–brain barrier dysfunction. Taken together, the minor photothrombosis model appears to provide a model useful for investigating novel treatments acting to improve *both mild ischemic damage and/or vascular injury*.

4.3. Recurrent minor stroke produced using repeated minor photothrombosis

Methods to produce overlapping recurrent mild ischemic insults have been limited to using multiple transient occlusions of the middle cerebral artery for relatively short intervals (Clark et al., 2012; Qiao et al., 2009). However, the middle cerebral artery occlusion model of recurrent stroke is challenging with multiple technically demanding invasive surgeries. We demonstrate that a minor recurrent stroke can be produced using multiple minor photothrombosis procedures that are relatively straight forward technically and less invasive than repeated microclip occlusion of the middle cerebral artery. However, because the strokes are small and somewhat variable in location, T_2 imaging using MRI is required to help identify the extent and location of the initial insult and is useful for assessing damage from the recurrent insult. Further reducing the variability of a single minor photothrombosis would facilitate T_2 guided study of the pathological effects and treatment of multiple mild ischemic injury associated with minor photothrombosis insults.

To conclude, the modified photothrombotic procedure presented in the present study will produce a minor stroke consisting of a small infarct in a region with marked Dw and T_2 hyperintensities. Adjacent to the very small infarct is a peri-infarct region of selective necrosis with modest T_2 changes that can guide selection of animals and help in assessment of novel treatments of the mild ischemic injury that occurs with TIA or in the penumbra region of a stroke. We also found that a recurrent insult is readily produced but T_2 imaging with MRI is important for assessing the extent of single and double mild ischemic injury.

Acknowledgements

Supported by grant MOP111037 from the Canadian Institutes for Health Research and a Brain Canada platform grant for the Experimental Imaging Centre.

References

Alaverdashvili, M., Moon, S.K., Beckman, C.D., Virag, A., Whishaw, I.Q., 2008. Acute but not chronic differences in skilled reaching for food following motor cortex devascularization vs. photothrombotic stroke in the rat. Neuroscience 157, 297–308.

Alaverdashvili, M., Paterson, P.G., Bradley, M.P., 2015. Laser system refinements to reduce variability in infarct size in the rat photothrombotic stroke model. J. Neurosci. Methods 247, 58–66.

Boquillon, M., Boquillon, J.P., Bralet, J., 1992. Photochemically induced, graded cerebral infarction in the mouse by laser irradiation evolution of brain edema. J. Pharmacol. Toxicol. Methods 27, 1–6.

Brazzelli, M., Chappell, F.M., Miranda, H., Shuler, K., Dennis, M., Sandercock, P.A., Muir, K., Wardlaw, J.M., 2014. Diffusion-weighted imaging and diagnosis of transient ischemic attack. Ann. Neurol. 75, 67–76.

Clark, D., Tuor, U.I., Thompson, R., Institoris, A., Kulynych, A., Zhang, X., Kinniburgh, D.W., Bari, F., Busija, D.W., Barber, P.A., 2012. Protection against recurrent stroke with resveratrol: endothelial protection. PLoS One 7, e47792.

Dietrich, W.D., Ginsberg, M.D., Busto, R., Watson, B.D., 1986. Photochemically induced cortical infarction in the rat. 1. Time course of hemodynamic consequences. J. Cereb. Blood Flow Metab. 6, 184–194.

Dietrich, W.D., Busto, R., Watson, B.D., Scheinberg, P., Ginsberg, M.D., 1987a. Photochemically induced cerebral infarction. II. Edema and blood-brain barrier disruption. Acta Neuropathol. 72, 326–334.

Dietrich, W.D., Watson, B.D., Busto, R., Ginsberg, M.D., Bethea, J.R., 1987b. Photochemically induced cerebral infarction. I. Early microvascular alterations. Acta Neuropathol. 72, 315–325.

Easton, J.D., Saver, J.L., Albers, G.W., Alberts, M.J., Chaturvedi, S., Feldmann, E., Hatsukami, T.S., Higashida, R.T., Johnston, S.C., Kidwell, C.S., Lutsep, H.L., Miller, E., Sacco, R.L., 2009. Definition and evaluation of transient ischemic attack: a scientific statement for healthcare professionals from the American Heart Association/American Stroke Association Stroke Council; Council on Cardiovascular Surgery and Anesthesia; Council on Cardiovascular Radiology and Intervention; Council on Cardiovascular Nursing; and the Interdisciplinary Council on Peripheral Vascular Disease. The American Academy of Neurology affirms the value of this statement as an educational tool for neurologists. Stroke 40, 2276–2293.

Ejaz, S., Emmrich, J.V., Sawiak, S.J., Williamson, D.J., Baron, J.C., 2015. Cortical selective neuronal loss, impaired behavior, and normal magnetic resonance imaging in a new rat model of true transient ischemic attacks. Stroke 46, 1084–1092.

Gu, W.G., Jiang, W., Brannstrom, T., Wester, P., 1999. Long-term cortical CBF recording by laser-Doppler flowmetry in awake freely moving rats subjected to reversible photothrombotic stroke. J. Neurosci. Methods 90, 23–32.

Harrison, T.C., Silasi, G., Boyd, J.D., Murphy, T.H., 2013. Displacement of sensory maps and disorganization of motor cortex after targeted stroke in mice. Stroke 44, 2300–2306.

Ito, D., Tanaka, K., Suzuki, S., Dembo, T., Fukuuchi, Y., 2001. Enhanced expression of Iba1, ionized calcium-binding adapter molecule 1, after transient focal cerebral ischemia in rat brain. Stroke 32, 1208–1215.

Jolkkonen, J., Jokivarsi, K., Laitinen, T., Grohn, O., 2007. Subacute hemorrhage and resolution of edema in Rose Bengal stroke model in rats coincides with improved sensorimotor functions. Neurosci. Lett. 428, 99–102.

Kao, Y.C., Li, W., Lai, H.Y., Oyarzabal, E.A., Lin, W., Shih, Y.Y., 2014. Dynamic perfusion and diffusion MRI of cortical spreading depolarization in photothrombotic ischemia. Neurobiol. Dis. 71C, 131–139.

Kernan, W.N., Ovbiagele, B., Black, H.R., Bravata, D.M., Chimowitz, M.I., Ezekowitz, M.D., Fang, M.C., Fisher, M., Furie, K.L., Heck, D.V., Johnston, S.C., Kasner, S.E., Kittner, S.J., Mitchell, P.H., Rich, M.W., Richardson, D., Schwamm, L.H., Wilson, J.A., 2014. Guidelines for the prevention of stroke in patients with stroke and transient ischemic attack: a guideline for healthcare professionals from the American Heart Association/American Stroke Association. Stroke 45, 2160–2236.

Lee, V.M., Burdett, N.G., Carpenter, T.A., Hall, L.D., Pambakian, P.S., Patel, S., Wood, N.I., James, M.F., 1996. Evolution of photochemically induced focal cerebral ischemia in the rat: magnetic resonance imaging and histology. Stroke 27, 2110–2118.

Li, R., Guo, J., Ma, X., Wang, S., Zhang, J., He, L., Gong, Q., Chen, H., 2015. Alterations in the gray matter volume in transient ischemic attack: a voxel-based morphometry study. Neurol. Res. 37, 43–49.

Moon, S.K., Alaverdashvili, M., Cross, A.R., Whishaw, I.Q., 2009. Both compensation and recovery of skilled reaching following small photothrombotic stroke to motor cortex in the rat. Exp. Neurol. 218, 145–153.

Paxinos, G., Watson, C., 1998. The Rat Brain in Sterotaxic Coordinates. Academic Press, New York.

Pevsner, P.H., Eichenbaum, J.W., Miller, D.C., Pivawer, G., Eichenbaum, K.D., Stern, A., Zakian, K.L., Koutcher, J.A., 2001. A photothrombotic model of small early ischemic infarcts in the rat brain with histologic and MRI correlation. J. Pharmacol. Toxicol. Methods 45, 227–233.

Pierpaoli, C., Righini, A., Linfante, I., Tao-Cheng, J.H., Alger, J.R., Di Chiro, G., 1993. Histopathologic correlates of abnormal water diffusion in cerebral ischemia: diffusion-weighted MR imaging and light and electron microscopic study. Radiology 189, 439–448.

Qiao, M., Foniok, T., Buist, R., Meng, S., Tomanek, B., Tuor, U.I., 2004. Cerebral blood flow response during hypoxia-ischemia and reperfusion differs in neonatal and juvenile rats. MAGMA 17, 117–124.

Qiao, M., Zhao, Z., Barber, P.A., Foniok, T., Sun, S., Tuor, U.I., 2009. Development of a model of recurrent stroke consisting of a mild transient stroke followed by a second moderate stroke in rats. J. Neurosci. Methods 184, 244–250.

Reeson, P., Tennant, K.A., Gerrow, K., Wang, J., Weiser, N.S., Thompson, K., Lockhart, K.L., Holmes, A., Nahirney, P.C., Brown, C.E., 2015. Delayed inhibition of VEGF signaling after stroke attenuates blood-brain barrier breakdown and improves functional recovery in a comorbidity-dependent manner. J. Neurosci. 35, 5128–5143.

Schmued, L.C., Hopkins, K.J., 2000. Fluoro-Jade B: a high affinity fluorescent marker for the localization of neuronal degeneration. Brain Res. 874, 123–130.

Schoknecht, K., Prager, O., Vazana, U., Kamintsky, L., Harhausen, D., Zille, M., Figge, L., Chassidim, Y., Schellenberger, E., Kovacs, R., Heinemann, U., Friedman, A., 2014. Monitoring stroke progression: in vivo imaging of cortical perfusion, blood-brain barrier permeability and cellular damage in the rat photothrombosis model. J. Cereb. Blood Flow Metab. 34, 1791–1801.

Schroeter, M., Franke, C., Stoll, G., Hoehn, M., 2001. Dynamic changes of magnetic resonance imaging abnormalities in relation to inflammation and glial responses after photothrombotic cerebral infarction in the rat brain. Acta Neuropathol. 101, 114–122.

Shih, A.Y., Blinder, P., Tsai, P.S., Friedman, B., Stanley, G., Lyden, P.D., Kleinfeld, D., 2013. The smallest stroke: occlusion of one penetrating vessel leads to infarction and a cognitive deficit. Nat. Neurosci. 16, 55–63.

Van Bruggen, N., Cullen, B.M., King, M.D., Doran, M., Williams, S.R., Gadian, D.G., Cremer, J.E., 1992. T2- and diffusion-weighted magnetic resonance imaging of a focal ischemic lesion in rat brain. Stroke 23, 576–582.

Verlooy, J., Van, R.J., Peersman, G., Van d, V., Van, D.B., Borgers, M., Selosse, P., 1993. Photochemically-induced cerebral infarction in the rat: comparison of NMR imaging and histologic changes. Acta Neurochir. (Wien) 122, 250–256.

Watson, B.D., Dietrich, W.D., Busto, R., Wachtel, M.S., Ginsberg, M.D., 1985. Induction of reproducible brain infarction by photochemically initiated thrombosis. Ann. Neurol. 17, 497–504.

Weiller, C., Willmes, K., Reiche, W., Thron, A., Isensee, C., Buell, U., Ringelstein, E.B., 1993. The case of aphasia or neglect after striatocapsular infarction. Brain 116 (Pt 6), 1509–1525.

Williams, D.S., Detre, J.A., Leigh, J.S., Koretsky, A.P., 1992. Magnetic resonance imaging of perfusion using spin inversion of arterial water. Proc. Natl. Acad. Sci. U. S. A. 89, 212–216 [published erratum appears in Proc. Natl. Acad. Sci. U. S. A. May 1, 1992, 89 (9), 4220].

Zhang, S., Boyd, J., Delaney, K., Murphy, T.H., 2005. Rapid reversible changes in dendritic spine structure in vivo gated by the degree of ischemia. J. Neurosci. 25, 5333–5338.

Zhang, S., Murphy, T.H., 2007. Imaging the impact of cortical microcirculation on synaptic structure and sensory-evoked hemodynamic responses in vivo. PLoS Biol. 5, e119.